

# A CIRCUMBINARY DISK MODEL FOR THE RAPID ORBITAL SHRINKAGE IN BLACK HOLE LOW-MASS X-RAY BINARIES

XIAO-TIAN XU<sup>1</sup> AND XIANG-DONG LI<sup>1,2</sup>

<sup>1</sup>*Department of Astronomy, Nanjing University, Nanjing 210046, China*

<sup>2</sup>*Key Laboratory of Modern Astronomy and Astrophysics (Nanjing University), Ministry of Education, Nanjing 210046, China*

(Received; Revised; Accepted)

Submitted to ApJ

## ABSTRACT

Several black hole low-mass X-ray binaries (BHLMXBs) show very fast orbital shrinkage, which is difficult to understand in the standard picture of the LMXB evolution. Based on the possible detection of a circumbinary (CB) disk in A0620-00 and XTE J1118+480, we investigate the influence of the interaction between a CB disk and the inner binary and calculate the evolution of the binary using the Modules for Experiments in Stellar Astrophysics. We consider two cases for the CB disk formation in which it is fed by mass loss during single outburst or successive outbursts in the LMXB. We show that when taking reasonable values of the initial mass and the dissipating time of the disk, it is possible to explain the fast orbital shrinkage in the BHLMXBs without invoking high mass transfer rate.

arXiv:1804.07914v1 [astro-ph.HE] 21 Apr 2018

## 1. INTRODUCTION

Black hole low-mass X-ray binaries (BHLMXBs), which are a subclass of X-ray binaries, consist of a stellar-mass BH accretor and a low-mass ( $\lesssim 1 M_{\odot}$ ) donor. There are 19 Galactic BHLMXBs dynamically confirmed (Remillard & McClintock 2006; McClintock & Remillard 2006; Casares & Jonker 2014). Most of the donors are dwarf stars with spectral types ranging from A2V to M1V. The masses of the BHs range from  $\sim 2.7 M_{\odot}$  to  $\gtrsim 15 M_{\odot}$ , and the orbital periods ( $P_{\text{orb}}$ ) are usually  $\lesssim 1$  day. All BHLMXBs are transients, alternating between long quiescence with X-ray luminosity  $L_X \sim 10^{30.5} - 10^{33.5} \text{ erg s}^{-1}$  and short outburst with  $L_X \sim 10^{37} - 10^{39} \text{ erg s}^{-1}$ . These different states are thought to be related to different accretion processes taking place in BHLMXBs. The quiescent and outburst states, which are characterized by low/hard and high/soft X-ray spectra, can be explained by an advection-dominated accretion flow (Narayan & Yi 1995; Abramowicz et al. 1995) and a optically thick, geometrically thin disk (Shakura & Sunyaev 1973), respectively; the transition between these states is usually thought to be driven by the change in the accretion rate (Esin, McClintock & Narayan 1997).

In the standard model of the formation of BHLMXBs (van den Heuvel 1983; Bhattacharya & van den Heuvel 1991; Tauris & van den Heuvel 2006), the progenitor of a BHLMXB is a binary with an extreme mass ratio in a relatively wide orbital (see Li 2015, for a review). After its main-sequence evolution, the primary star expands rapidly and overflows its Roche lobe. Due to the high mass ratio the mass transfer is dynamically unstable and the transferred material engulfs the secondary star. Then, the system enters the common envelope (CE) phase (Paczynski 1976). The CE evolution yields a close binary system or merger of the two stars, depending on the dissipation process in the stellar envelope of the primary star. If the binary can survive the CE phase, the secondary still remains in the main-sequence and the primary star evolves into a naked core, which finally experiences core-collapse with the formation of a BH. A natal kick may be imparted to the BH during the collapse. If the binary can survive, the subsequent evolution is driven by either nuclear evolution of the secondary star or magnetic braking (MB) and gravitational radiation (GR). Once the orbit is narrow enough for the onset of mass transfer, the binary behaves as a LMXB.

Orbital evolution can provide useful probe of the mass transfer processes in BHLMXBs. However, it is challenging to measure the derivative ( $\dot{P}_{\text{orb}}$ ) of the orbital period in BHLMXBs. Recently, González Hernández et al. (2012, 2014, 2017) reported the  $\dot{P}_{\text{orb}}$  measurements of three BHLMXBs (A0620-00, XTE J1118+480 and Nova Muscae 1991) by using the Doppler shift of the companion's spectral lines, and found that these BHLMXBs are experiencing extremely rapid orbital shrinkage (see Table 1 for a summary of the observed parameters). The rates of orbital decay exceed the expectation of the traditional theory invoking angular momentum loss (AML) caused by MB and GR by around 1 – 2 orders of magnitude. If the orbital shrinkage is caused by mass loss, then the large value of  $|\dot{P}_{\text{orb}}|$  requires that the donor be losing mass at a very high rate so the binary would be bright in X-ray. However, the observed X-ray luminosities of these BHLMXBs are all quite low: their Eddington-scaled luminosities are about  $10^{-3} - 10^{-2}$  (McClintock & Remillard 2006; Wu et al. 2010).

This exotic behavior challenges our understanding about the evolution of BHLMXBs. Several scenarios were suggested in the literature. (1) A massive planet orbiting the binary may be responsible for the orbital shrinkage (Peuten et al. 2014; Iaria et al. 2015; Jain et al. 2017). In this scenario, the orbit should experience a series of shrinkage and expansion due to the motion of the third-body. However, currently there is no direct observational indication of the existence of a third-body in these BHLMXBs, and more observations are needed to test this idea. (2) Some authors proposed that anomalous magnetic activity of the low-mass donor may cause the rapid orbital decay (i.e., MB with strong surface magnetic field of order 1 kG: Justham et al. 2006 or the Applegate mechanism: González Hernández et al. 2014). Evolutionary studies showed that the effective temperatures of the donor stars are higher than observed in the former model (Justham et al. 2006), and it remains to see whether the internal energy budget of the low-mass donor star is sufficient to produce the observed orbital period change with the Applegate mechanism in LMXBs (Patruno et al. 2016). (3) Based on the fact that there is a circumbinary (CB) disk detected in both A0620-00 and XTE J1118+480 with mass  $\sim 10^{22} - 10^{24} \text{ g}$  (Muno & Mauerhan 2006), Chen & Li (2015) investigated the AM transfer between the CB disk and the binary caused by mass flow between them. The mass flow itself can take away AM from the binary, causing the orbit to shrink. However, to reach the observed shrinking rate, the expected mass of the CB disk is six orders of magnitude higher than observed.

In this paper, we investigate an alternative CB disk model, considering gravitational resonant interaction between the disk and the binary. Resonant interaction between a CB disk and the inner binary has been already investigated in binary systems, and it has been demonstrated that a CB disk is able to effectively extract AM from the binary (Artymowicz et al. 1991; Lubow & Artymowicz 1996, 2000; Dermine et al. 2013). However, it is still open whether

this mechanism can account for the observation of BHLMXBs. The rest of this paper is organized as follows. We describe the model for the CB disk-binary interaction and the binary orbital evolution in section 2. Then we perform numerical calculation of the binary evolution with different initial parameters and evolutionary laws of the CB disk, and compare the results with observations. In section 4, we summarize our work.

## 2. MODEL

In this work we assume that the observed orbital shrinkage is related to the formation and evolution of a CB disk, which originates from sporadic mass loss process during outburst(s) of the BHLMXBs. So, before investigating the influence of the disk, we need to follow the long-term evolution of the binary and set the initial condition at the onset of the CB disk formation. We calculate the BHLMXB evolution with the Modules for Experiments in Stellar Astrophysics (MESA; version number 9575) (Paxton et al. 2011, 2013, 2015). The physical considerations are described as below.

The Roche-lobe  $R_{L,2}$  of the donor is evaluated with the formula proposed by Eggleton (1983),

$$\frac{R_{L,2}}{a} = \frac{0.49q^{2/3}}{0.6q^{2/3} + \ln(1 + q^{1/3})}, \quad (1)$$

where  $q = M_2/M_{\text{BH}}$  is the mass ratio of the donor mass  $M_2$  and the BH mass  $M_{\text{BH}}$ , and  $a$  is the orbital separation. We adopt the Ritter scheme in MESA to calculate the mass transfer rate via Roche-lobe overflow (Ritter 1988),

$$-\dot{M}_2 = \dot{M}_{2,0} \exp\left(-\frac{R_2 - R_{L,2}}{H}\right), \quad (2)$$

where  $R_2$  is the radius of the donor,  $H$  is scale height of the atmosphere evaluated at the surface of the donor star, and

$$\dot{M}_{2,0} = \frac{1}{e^{1/2}} \rho c_{\text{th}} Q, \quad (3)$$

where  $\rho$  and  $c_{\text{th}}$  are the mass density and the sound speed at the surface of the star respectively, and  $Q$  is the cross section of the mass flow via the L1 point. We assume that the accretion rate onto BH is limited by the Eddington accretion rate  $\dot{M}_{\text{Edd}}$ , i.e.,

$$\dot{M}_{\text{BH}} = \min(|\dot{M}_2|, \dot{M}_{\text{Edd}}), \quad (4)$$

and  $\dot{M}_{\text{Edd}}$  is given by (Podsiadlowski et al. 2003),

$$\dot{M}_{\text{Edd}} = 2.6 \times 10^{-7} M_{\odot} \text{yr}^{-1} \left(\frac{M_{\text{BH}}}{10M_{\odot}}\right) \left(\frac{\eta}{0.1}\right)^{-1} \left(\frac{1+X}{1.7}\right)^{-1}, \quad (5)$$

where  $X$  is the hydrogen mass fraction of the accreted material, and  $\eta$  is the efficiency of energy conversion. The excess matter is assumed to be ejected from the binary in the form of isotropic wind.

We divide the binary evolution into two phases: the pre-CB disk phase and the CB disk phase. The pre-CB disk phase starts from the birth of a BH in a binary with a low-mass zero-age main-sequence star, and terminates at the observed  $P_{\text{orb}}$ , where we assume a CB disk is formed. We try to match the observed  $P_{\text{orb}}$ ,  $M_2$  and the effective temperature  $T_{\text{eff}}$  of the donor by varying the initial parameters. In the calculation we adopt the standard AML processes including MB, GR, and mass loss via isotropic wind. The total AML rate in the pre-CB disk phase is given by

$$\dot{J}_{\text{orb}} = \dot{J}_{\text{GR}} + \dot{J}_{\text{MB}} + \dot{J}_{\text{ML}}, \quad (6)$$

where  $J_{\text{orb}}$  is the orbital AM of the binary

$$J_{\text{orb}} = M_2 M_{\text{BH}} \left(\frac{Ga}{M_2 + M_{\text{BH}}}\right)^{1/2}, \quad (7)$$

and  $\dot{J}_{\text{orb}}$  is its time derivative. On the right-hand-side of Eq. (6),  $\dot{J}_{\text{GR}}$  is the AML rate caused by GR (Landau & Lifshitz 1975)

$$\dot{J}_{\text{GR}} = -\frac{32}{5c^5} \left(\frac{2\pi G}{P_{\text{orb}}}\right)^{7/3} \frac{(M_2 M_{\text{BH}})^2}{(M_{\text{BH}} + M_2)^{2/3}}, \quad (8)$$

where  $c$  is the speed of light and  $G$  is the gravitational constant. The  $\dot{J}_{\text{MB}}$  term is related to MB and described by the following formula (Verbunt & Zwaan 1981; Rappaport et al. 1983),

$$\dot{J}_{\text{MB}} = -3.8 \times 10^{-30} M_2 R_2^4 \omega_{\text{orb}}^3 \text{ dyn cm}, \quad (9)$$

where  $\omega_{\text{orb}}$  is the angular velocity of the binary. Finally  $\dot{J}_{\text{ML}}$  represents the AML rate by isotropic wind from the BH,

$$\dot{J}_{\text{ML}} = -(|\dot{M}_2| - \dot{M}_{\text{BH}}) a_{\text{BH}}^2 \omega_{\text{orb}}, \quad (10)$$

where  $a_{\text{BH}}$  is the distance between the BH and the center of mass of the binary.

We then use the results of the pre-CB disk evolution as the input for the calculation of the CB disk evolution. The CB disk phase is related to the evolution with the effect of the CB disk taken into account. The total AML rate in this phase is given by

$$\dot{J}_{\text{orb}} = \dot{J}_{\text{GR}} + \dot{J}_{\text{MB}} + \dot{J}_{\text{ML}} + \dot{J}_{\text{CB}}, \quad (11)$$

where the  $\dot{J}_{\text{CB}}$  term results from the resonant interaction between the CB disk and the binary, and is evaluated by (Lubow & Artymowicz 1996)

$$\frac{\dot{J}_{\text{CB}}}{J_{\text{orb}}} = -\frac{l}{m} \frac{M_{\text{CB}}}{\mu} \alpha \left( \frac{H}{R} \right)^2 \frac{a}{R} \frac{2\pi}{P_{\text{orb}}}, \quad (12)$$

where  $l$  and  $m$  are integers describing the binary potential,  $M_{\text{CB}}$  is the mass of CB disk,  $\mu$  is the reduced mass of the binary

$$\mu = \frac{M_2 M_{\text{BH}}}{M_2 + M_{\text{BH}}}, \quad (13)$$

$\alpha$  is the viscosity parameter of the disk (Shakura & Sunyaev 1973), and  $R$  is the half-AM radius of the CB disk  $R = \sqrt{r_{\text{in}} r_{\text{out}}}$  ( $r_{\text{in}}$ : the inner radius of the CB disk;  $r_{\text{out}}$ : the outer radius of the CB disk).

Our input parameters are described as follows. Assuming that the non-axisymmetric potential perturbations are small, we take  $l = m = 1$ . We adopt typical values for the viscosity in the CB disk, i.e.,  $\alpha = 0.01 - 0.1$ . Dullemond et al. (2001) constructed a model for irradiated dusty CB disk. According to their study, the thickness near the inner edge of the disk is  $H/R = 0.1 - 0.25$ , so we set  $(H/R)^2 = 1/30$ . Miranda & Lai (2015) investigated the tidal truncation between the CB disk and the inner binary. Assuming the balance between resonant torque and viscous torque as the truncation criterion, they found that the inner radius of the CB disk is  $1.5a < r_{\text{in}} < 3.5a$ . We accordingly assume the CB disk to extend from  $r_{\text{in}} = 2.5a$ . The outer radius of the CB disk  $r_{\text{out}}$  is assumed to be  $r_{\text{out}} = (10 - 100)a$ .

Recently, Jiang et al. (2017) investigated the feasibility of a CB disk in understanding the orbital evolution of the ultra-compact X-ray binary 4U 1820-303, which harbors a neutron star. They assume that the CB disk originates from the material ejected by the superburst from the neutron star. In BHLMXBs, the mass ejection feeding the CB disk may be generated by the outburst triggered by the instability of accretion disk, or the disk wind driven by the magnetic pressure (see Yuan & Narayan 2014, for a review). Meanwhile, it is still under debate whether the observed orbital decay is a short-term or a long-term phenomenon. Thus, we take into account two cases, in which the CB disk is fed either by one specific outburst or by a series of outbursts. For the evolution of a debris disk, one can solve the disk structure equations to obtain its self-similar solutions (Pringle 1974; Cannizzo et al. 1990). The total mass of the disk evolves as

$$M_{\text{CB}} = M_{\text{CB},0} \left( 1 + \frac{t}{t_{\text{vis},0}} \right)^{-n}, \quad (14)$$

where  $M_{\text{CB},0}$  is the initial mass of the disk,  $t_{\text{vis},0}$  is the viscous timescale at the formation of the disk, and  $n$  is a constant determined by opacity laws. Let  $r_0$  be the initial radius of the disk, we can estimate the viscous timescale to be

$$t_{\text{vis},0} \sim \frac{r_0}{v_r} \sim 1 \text{ yr} \left( \frac{\alpha}{0.1} \right)^{-1} \left( \frac{r_0}{10a} \right)^{3/2}, \quad (15)$$

where  $v_r$  is the radial velocity of the disk material (here the orbital period is taken to be 0.5 d). Considering the possible range of  $\alpha$  and  $r_0$ , we take  $t_{\text{vis},0} = 1, 10, \text{ and } 30 \text{ yr}$  in our calculations. For bound-free dominating opacities, one can obtain  $n = 1/4$  (Cannizzo et al. 1990). However, Ertan et al. (2009) pointed out that the disk may dissipate more quickly after the the disk becomes sufficiently cool and passive. In this case there is no analytic solution the evolution of the disk mass. We tentatively adopt  $n = 3/4$  according to their numerically calculated results.

### 3. RESULTS

#### 3.1. Pre-CB disk evolution

In this subsection, we present the results in the pre-CB disk phase by calculating a number of evolutions with different initial values of  $M_2$  and  $P_{\text{orb}}$ . Several authors have theoretically investigated the properties of the donors in BHLMXBs (e.g., Podsiadlowski et al. 2003; Ivanova 2006; Justham et al. 2006; Yungelson & Lasota 2008; Chen & Li 2015; Fragos & McClintock 2015; Wang et al. 2016). In Table 1, We list the observed parameters of the three BHLMXBs. It is noted that Wu et al. (2015) obtained the effective temperatures  $T_{\text{eff}}$  of the donor stars by using the TDR-value method (Tonry & Davis 1979) to fit their spectral types, González Hernández et al. (2004, 2006) studied the emission lines of A0620-00 and XTE J1118-480 and obtained the effective temperatures by Monte-Carlo simulation, and Fragos & McClintock (2015) used an empirical relation to convert the spectral type into the effective temperature. In our study, we adopt the values of  $T_{\text{eff}}$  reported by Fragos & McClintock (2015), and ignore the possible X-ray irradiation from the BH when comparing theory with observation. The reasons are that the effect of irradiation on the donor star is still highly uncertain and all of the three binaries are transients with very low X-ray luminosities. Table 2 lists the typical parameters selected from our calculations for the three LMXBs after the CE phase, which can lead to the current evolutionary stage.

Example evolutionary tracks during the pre-CB disk phase are presented in Fig. 1. The left, middle, and right rows correspond to the evolutions of A0620-00, XTE J1118-480, and Nova Muscae 1991, respectively. The blue solid line in each panel depicts  $T_{\text{eff}}$ ,  $P_{\text{orb}}$ ,  $R_2$ , Age and  $\dot{M}_2$  as a function of  $M_2$ . The shaded areas, the black rectangles, and the black horizontal lines denote the observational constraints on  $M_2$ ,  $T_{\text{eff}}$  and  $P_{\text{orb}}$ , respectively. It can be seen that our model can match the observations of A0620-00 and XTE J1118+480 fairly well, but in the case of Nova Muscae 1991, the modeled  $T_{\text{eff}}$  is always slightly higher than observed. The binaries all show long-term orbital decay driven mainly by MB, and the mass transfer rates are relative low ( $< 10^{-9} M_{\odot} \text{yr}^{-1}$ ).

#### 3.2. CB disk evolution

##### 3.2.1. CB disk fed by single outburst

In this subsection, we present the results of the evolution with the assumption that the CB disk is formed by mass ejection in single outburst. Firstly we show the evolution of  $|\dot{P}_{\text{orb}}|$  and  $\log(|\dot{M}_2|)$  during a period of  $10^4$  yr in Figs. 2 and 3 with  $n = 1/4$  and  $3/4$ , respectively. The input parameters ( $\alpha$ ,  $r_0$ ,  $t_{\text{vis},0}$ ,  $M_{\text{CB},0}$ ) for each panel are listed in Table 3. The blue solid lines represent the evolution of  $|\dot{P}_{\text{orb}}|$  with  $\dot{P}_{\text{orb}} < 0$ , and the green solid lines the evolution of  $|\dot{M}_2|$ , respectively. For comparison, we also plot the evolution of  $|\dot{P}_{\text{orb}}|$  and  $|\dot{M}_2|$  in the absence of a CB disk with the blue and green dashed lines, respectively. The shaded areas denote the observed range of  $\dot{P}_{\text{orb}}$ .

The general feature in Figs. 2 and 3 is that, when the system enters the CB disk phase, the value of  $-\dot{P}_{\text{orb}}$  increases immediately, and then decreases roughly on a viscous timescale. Theoretically it is possible to explain the rapid orbital shrinkage of the BHLMXBs with reasonable values of  $M_{\text{CB},0}$  and  $t_{\text{vis},0}$ . It is known that a rapid orbital decay can accelerate mass loss from the donor, consequently enhance the X-ray luminosity (Justham et al. 2006; Chen & Li 2015). However, observationally the three BHLMXBs are all faint sources. Figs. 2 and 3 show that there is a time delay between the increase in  $|\dot{P}_{\text{orb}}|$  and  $|\dot{M}_2|$ , which means that it takes the donor a relaxation time to adjust its structure in response to the increase in  $|\dot{P}_{\text{orb}}|$ . In the case of  $n = 3/4$  the change of  $|\dot{M}_2|$  is much smaller than in the case of  $n = 1/4$  because of more rapid disk dissipation. Thus, it is possible that the formation of CB disk can lead to a rapid orbital decay without changing  $|\dot{M}_2|$  significantly.

Then, we study the effect of  $M_{\text{CB}}$  on the CB disk evolution within a relatively long time of  $10^6$  yr. Here we take  $n = 3/4$ . The results are shown in Figs. 4, 5, and 6 for A0620-00, XTE J1118+480, and Nova Muscae 1991, respectively. In each figure, the left and right columns depict the evolution of  $|\dot{P}_{\text{orb}}|$  (blue solid and dashed lines for  $|\dot{P}_{\text{orb}}|$  with and without a CB disk respectively) and  $|\dot{M}_2|$ . For each BHLMXB, we adopt the same parameters in Table 3 but adding a factor  $\zeta$  to  $M_{\text{CB},0}$  with  $\zeta = (4, 1, 4^{-1}, 4^{-2}, 4^{-3}, 4^{-4})$ . corresponding to the six evolutionary tracks in each panel from top to bottom, respectively.

In the case of A0620-00, the CB disk can lead to orbital decay for a time of a few  $10^4$  yr. The orbital decay with  $\zeta = (4, 1, 4^{-1})$  is fast enough to match the observed value. The more massive the CB disk and the longer the initial viscous time, the longer time for the orbital shrinkage, consequently the higher mass loss rate. In the case of  $t_{\text{vis},0} = 30$  yr and  $\zeta = 4$ , the mass transfer can even cause the orbital period to expand for some time, which is depicted with the red line in the lower left panel. After that the orbital period decreases again due to AML by MB and GR.

The general picture of the evolution of XTE J1118+480 is similar to that of A0620-00. The donor of XTE J1118+480 is older and less massive, and MB in the donor has already been turned off because of the absence of the radiative core. Thus, the mass loss process of the donor is more sensitive to the change in  $\dot{P}_{\text{orb}}$ . Before the formation of the CB disk,  $|\dot{M}_2|$  is very low ( $< 10^{-10} M_{\odot} \text{yr}^{-1}$ ). When entering the CB disk phase, the rapid orbit shrinkage causes a higher enhancement of  $|\dot{M}_2|$  than in A0620-00. Compared with the other two sources, the donor of Nova Muscae 1991 is younger and more massive. Thus, before the formation of the CB disk,  $|\dot{M}_2|$  is relatively high. The donor responds more quickly to the change in  $\dot{P}_{\text{orb}}$ , leading to shorter duration of the  $|\dot{M}_2|$ -enhancement.

### 3.2.2. CB disk fed by successive outbursts

In this subsection we consider the alternative case that the CB disk is fed by a series of successive mass ejection processes from the binary. We assume that the lost material during the outbursts with a duty cycle of 1/200, which is typical in BHLMXBs, is repeatedly added to the CB disk, which then dissipates on a viscous timescale. As an illustration, we present the evolution of  $|\dot{P}_{\text{orb}}|$  and  $|\dot{M}_2|$  within  $2 \times 10^6$  yr in Fig. 7. Here we adopt the input parameters in the middle row in Table 3 with  $n = 3/4$ . The upper, middle, and lower panels depict the results for A0620-00, XTE J1118+480, and Nova Muscae 1991, respectively. The blue and red solid lines represent the evolution of  $|\dot{P}_{\text{orb}}|$  with  $\dot{P}_{\text{orb}} < 0$  and  $> 0$  respectively, and the green line represents the evolution of  $|\dot{M}_2|$ . The shaded areas denote the observed range of  $\dot{P}_{\text{orb}}$ . A zoom-in of the features in Fig. 7 is shown in Fig. 8, where the left and right panels demonstrate the evolution in  $0 - 50000$  yr and in  $10^6 - (10^6 + 50000)$  yr, respectively.

As we demonstrate in last subsection, in the case of single outburst-induced CB disk, there is a time delay between the increases in  $|\dot{P}_{\text{orb}}|$  and in  $|\dot{M}_2|$ , and after the dissipation of the CB disk the donor takes a relatively long relaxation time ( $> 10^4$  yr) to return to the previous evolutionary path. For successive outbursts the donor does not have enough time to adjust its structure in responding to the dissipation of the CB disk before the next cycle of mass feeding. Consequently,  $|\dot{M}_2|$  increases within the initial several cycles, during which the orbital period keeps decreasing. At some point,  $\dot{M}_2$  is high enough to induce orbital expansion after the dissipation of the CB disk in each cycle, which limits the increasing trend of  $|\dot{M}_2|$ . The orbital shrinkage and expansion take place in turn, and  $|\dot{M}_2|$  reaches a relatively stable value. For A0620-00, XTE J1118+480, and Nova Muscae 1991, it is  $< 5 \times 10^{-10} M_{\odot} \text{yr}^{-1}$ ,  $< 5 \times 10^{-10} M_{\odot} \text{yr}^{-1}$ , and  $< 1.5 \times 10^{-9} M_{\odot} \text{yr}^{-1}$ , respectively. From Figs. 7 and 8, the time percentages for the orbital decay rates larger than observed ones are 0.50%, 0.31% and 0.046% for A0620-00, XTE J1118+480, and Nova Muscae 1991, respectively. Obviously these values can be increased considerably if taking larger  $t_{\text{vis},0}$  and/or smaller  $n$ . Therefore, a CB disk fed by successive outburst may also explain the rapid orbital shrinkage while keeping  $|\dot{M}_2|$  relatively low.

We also plot the evolution of  $P_{\text{orb}}$  in Fig. 9, in which the upper, middle, and lower panels correspond to A0620-00, XTE J1118+480, and Nova Muscae 1991, respectively. The blue solid and dashed lines represent the evolution with and without a CB disk. This figure shows that, although both orbital shrinkage and expansion take place in the CB disk case, the former dominates the long-term evolution, and results in a orbital decay faster than driven only by MB and GR.

## 4. DISCUSSION

The rapid orbital shrinkage in the three BHLMXBs remains to be a puzzle in the traditional framework of LMXB evolution. Besides the dynamical interaction with a third-body, one of the most natural explanations is efficient AML associated with mass loss. However, this scenario usually induces rapid mass transfer at a rate higher than observed. Meanwhile, infrared observations point to the possible existence of a CB disk around the binaries but strongly constrain its mass (Muno & Mauerhan 2006).

In this work we take into account the effect of the resonant interaction between the CB disk and the inner binary, assuming that the CB disk originates from outburst(s) triggered by some instability in the BH accretion disk. Because the origin and evolution of the CB disk is still uncertain, we consider that the disk is fed by either single outburst or successive outbursts, and examine how the interaction changes with initial mass and lifetime of the disk. Our results show that the resonant interaction between the CB disk and the binary may explain the observed  $\dot{P}_{\text{orb}}$  with the disk mass comparable with observations and no significant change in  $\dot{M}_2$ .

In this work we assume that the CB disk originates from mass ejection during outburst(s) which may be caused by thermal instability in the accretion disk around the BH when the accretion rate is lower than a critical value (Lasota 2001). Under this condition the successive outburst model may be more viable than the single outburst model since all transient BHLMXBs are believed to be recurrent. However, it is difficult to definitely determine when the disk starts to be unstable and how much mass ejected during a specific outburst goes into the CB disk, so we arbitrarily

assume that the CB disk is formed at current time. With this approach we can focus on the effect of the CB disk on the orbital evolution with the binary parameters compatible with observations. If the CB disk was formed at an earlier time, the long-term (CB disk-assisted) orbital decay would proceed at a higher rate than only with MB and GR taken into account, then a smaller initial donor mass would be required.

For the disk-binary interaction, dynamical friction was also proposed in the literature (e.g., Syer & Clarke 1995; Ivanov et al. 1999). Under this circumstance, the secondary is assumed to be embedded and open a gap in an accretion disk surrounding the primary. The width of the gap is assumed to remain considerably smaller than the orbital radius of the secondary to guarantee dynamical interaction. It was found that the timescale of orbital shrinkage is much longer than the local viscous timescale of the disk if the disk mass is significantly smaller than the secondary's mass. The condition is different for the CB disk case. Here the CB disk, with a central cavity, is coupled with the inner binary via long-range resonant interaction (Goldreich & Tremaine 1979; Lubow & Artymowicz 1997). Rafikov (2016) recently investigated the angular momentum exchange between a post-main-sequence binary and a viscously evolving CB disk. It can be shown that the torque acting on the binary derived by Rafikov (2016) is consistent with Eq. (12) in our work. Therefore, while the mass of CB disk is significantly lower than that of the secondary, it is capable of efficiently extracting angular momentum via resonant interaction.

We note that orbital changes have also been observed in neutron star LMXBs. For example, SAX J1808.4-3658, 2A 1822-371, and SAX J1748.9-2021 show orbital expansion (Hartman et al. 2008; Burderi et al. 2010; Sanna et al. 2016), while X1658-298 and AX J1745.6-2901 (Wachter et al. 2000; Ponti et al. 2016) show orbital shrinkage. Since these LMXBs are all short-period binaries that share some similarities with the three BH binaries, the implication is that more than one kinds of mechanisms might be at work in LMXBs. To account for the observed period change, the Applegate mechanism requires a  $\sim 1$  KG surface magnetic field for the donor star, and the CB disk model predicts that the eccentricity could evolve with the orbital change (Dermine et al. 2013; Antoniadis 2014; Rafikov 2016). More detailed observations are expected to provide stringent constraint on the binary evolution and discriminate various kinds of models.

We are grateful to the referee for helpful comments. This work was supported by the National Key Research and Development Program of China (2016YFA0400803), and the Natural Science Foundation of China under grant numbers 11773015, 11133001 and 11333004.

## REFERENCES

- Abramowicz, M. A., Chen, X., Kato, S., et al. 1995, *ApJL*, 438, L37
- Antoniadis, J., 2014, *ApJL*, 797, L24
- Alexander, R. D., Clarke, C. J., & Pringle, J. E., 2006, *MNRAS*, 369, 229
- Artymowicz, P., Clarke, C. J., Lubow, S. H., et al. 1991, *ApJL*, 370, L35
- Bhattacharya, D. and van den Heuvel, E. P. J., 1991, *PhR*, 203, 1
- Burderi, L., Di Salvo, T., Riggio, A., et al. 2010, *A&A*, 515, 44
- Cannizzo, J. K., Lee, H. M., & Goodman, J. 1990, *ApJ*, 351, 38
- Casares, J. and Jonker, P. G., 2014, *SSRv*, 183, 223
- Chen, W.-C. and Li, X.-D., 2015, *A&A*, 583, A108
- Chesneau, O., 2013, in *The Environments of the Sun and the Stars*, Vol. 857, ed. J.-P. Rozelot & C. Neiner (Berlin: Springer), 239
- Dermine, T., Izzard, R. G., Jorissen, A., et al. 2013, *A&A*, 551, A50
- Dullemond, C. P., Dominik, C. & Natta, A., 2001, *ApJ*, 560, 957
- Eggleton, P. P., 1983, *ApJ*, 268, 368
- Ertan, Ü., Ekşi, K. Y., Erkut, M. H. et al. 2009, *ApJ*, 702, 1309
- Esin, A. A., McClintock, J. E. & Narayan, R., 1997, *ApJ*, 489, 865
- Fragos, T. & McClintock, J. E., 2015, *ApJ*, 800, 17
- Frank, J., King, A., & Raine, D. J. 2002, *Accretion Power in Astrophysics: Third Edition* (Cambridge University Press), 55
- Goldreich, P. & Tremaine, S., 1979, *ApJ*, 233, 857
- González Hernández, J. I., Casares, J., Rebolo, R., et al. 2011, *ApJ*, 738, 95
- González Hernández, J. I., Rebolo, R., Israelian, G., et al. 2004, *ApJ*, 609, 988
- González Hernández, J. I., Rebolo, R. & Casares, J., 2012, *ApJL*, 744, L25
- González Hernández, J. I., Rebolo, R. & Casares, J., 2014, *MNRAS*, 438, L21

- González Hernández, J. I., Rebolo, R., Israelian, G. et al. 2006, *ApJL*, 644, L49
- González Hernández, J. I., Suárez-Andrés, L., Rebolo, R., et al. 2017, *MNRAS*, 465, L15
- Hartman, J. M., Patruno, A., Chakrabarty, D., et al. 2008, *ApJ*, 675, 1468
- Haswell, C. A., Hynes, R. I., King, A. R. & Schenker, K., 2002, *MNRAS*, 332, 928
- Iaria, R., Di Salvo, T., Gambino, A. F., et al. 2015, *A&A*, 582, A32
- Ivanov, P. B., Papaloizou, J. C. B., Polnarev, A. G., 1999, *MNRAS*, 307, 79
- Ivanova, N., 2006, *ApJL*, 653, L137
- Jain, C., Paul, B., Sharma, R., et al. 2017, *MNRAS*, 468, L118
- Justham, S., Rappaport, S. & Podsiadlowski, P., 2006, *MNRAS*, 366, 1415
- Jiang, L. , Chen, W.-C. & Li, X.-D., 2017, *ApJ*, 837, 64
- Landau, L. D. & Lifshitz, E. M. 1975, *The Classical Theory of Fields* (4th ed.; Oxford: Pergamon)
- Lasota, J. P. 2001, *NewAR*, 45, 449
- Li, X.-D., 2015, *NewAR*, 64, 1
- Lubow, S. H. and Artymowicz, P., 1996, in *NATO ASIC Proc. 477, Evolutionary Processes in Binary Stars*, ed. R. A. M. J. Wijers, M. B. Davies, & C. A. Tout (Dordrecht: Kluwer), 53
- Lubow, S. H. & Artymowicz, P., 1997, in *IAU Colloq. 163: Accretion Phenomena and Related Outflows*, ed. Wickramasinghe, D. T., Bicknell, G. V. & Ferrario, L., 121, 503
- Lubow, S. H. and Artymowicz, P., 2000, in *Protostars and Planets IV*, ed. V. Mannings, A. P. Boss, & S. S. Russell (Tucson, AZ: Univ. Arizona Press), 731
- McClintock, J. E. & Remillard, R. A., 2006, A-Xiv e-prints [0306213]
- Miranda, R. & Lai, D., 2015, *MNRAS*, 452, 2396
- Muno, M. P. and Mauerhan, J., 2006, *ApJL*, 648, 135
- Narayan, R. & Yi, I., 1995, *ApJ*, 452, 710
- Neilsen, J., Steeghs, D. & Vrtilak, S. D., 2008, *MNRAS*, 384, 849
- Owen, J. E., Clarke, C. J., & Ercolano, B., 2012, *MNRAS*, 422, 1880
- Paczynski, B., 1976, In: Eggleton, P. and Mitton, S. and Whelan, J. (Eds.), *IAU Symposium, Structure and Evolution of Close Binary Systems*, 73, 75
- Patruno, A., Jaodand , A., Kuiper, L. et al. 2016, submitted to *ApJ*, arXiv:1611.06023
- Paxton, B., Bildsten, L., Dotter, A., et al. 2011, *ApJS*, 192, 3
- Paxton, B., Cantiello, M., Arras, P., et al. 2013, *ApJS*, 208, 4
- Paxton, B., Marchant, P., Schwab, J., et al. 2015, *ApJS*, 220, 15
- Peuten, M., Brockamp, M., Küpper, A. H. W. & Kroupa, P., 2014, *ApJ*, 795, 116
- Podsiadlowski, P., Rappaport, S. & Han, Z., 2003, *MNRAS*, 341, 385
- Ponti, G., De, K., Munoz-Darias, T., Stella, L., & Nandra, K. 2016, *MNRAS*, 464, 840
- Portegies Zwart, S. F., Verbunt, F. & Ergma, E., 1997, *A&A*, 321, 207
- Pringle, J. E. 1974, PhD thesis, Cambridge Univ.
- Rafikov, R. R., 2016, *ApJ*, 830, 8
- Rappaport, S. and Verbunt, F. and Joss, P. C., 1983, *ApJ*, 275, 713
- Remillard, R. A. & McClintock, J. E., 2006, *ARA&A*, 44, 49
- Ritter, H., 1988, *A&A*, 202, 93
- Sanna, A., Burderi, L., Riggio, A., et al. 2016, *MNRAS*, 459, 1340
- Shakura, N. I. & Sunyaev, R. A. 1973, *A&A*, 24, 337
- Syer, D. & Clarke, C. J., 1995, *MNRAS*, 277, 758
- Tauris, T. M. and van den Heuvel, E. P. J., 2006, In: Lewin, W., van der Klis, M. (Eds.), *Compact Stellar X-ray Sources*. Cambridge Univ. Press, Cambridge, p. 623.
- Tonry, J. & Davis, M., 1979, *AJ*, 84, 1151
- van den Heuvel, E. P. J., 1983 In: Lewin, W. H. G. & van den Heuvel, E. P. J. (Eds.), *Accretion-driven Stellar X-ray Sources*. Cambridge University Press, p. 303.
- Verbunt, F. and Zwaan, C., 1981 *A&A*, 100, L7
- Wachter, S., Smale, A. P., & Baily, C. 2000, *ApJ*, 534, 367
- Wang, C., Jia, K. & Li, X.-D, 2016, *MNRAS*, 457, 1015
- Wu, J., Orosz, J. A., McClintock, J. E., et al. 2015, *ApJ*, 806, 92
- Wu, J., Orosz, J. A., McClintock, J. E. et al. 2016, *ApJ*, 825, 46
- Wu, Y. X., Yu, W., Li, T. P., Maccaronae, T. J., & Li, X. D. 2010, *ApJ*, 718, 620
- Yuan, F. & Narayan, R., 2014, *ARA&A*, 52,529
- Yungelson, L. R., & Lasota, J.-P., 2008, *A&A*, 488, 257

**Table 1.** Observed parameters of the BHLMBs

Parameter <sup>a</sup>	Nova Muscae 1991	Ref. <sup>b</sup>	XTE J1118+480	Ref. <sup>b</sup>	A0620-00	Ref. <sup>b</sup>
$M_{\text{BH}}$ ( $M_{\odot}$ )	$11.0^{+2.1}_{-1.4}$	[1]	$7.46^{+0.34}_{-0.69}$	[2]	$6.61^{+0.23}_{-0.17}$	[2]
$M_2$ ( $M_{\odot}$ )	$0.89 \pm 0.18$	[1]	$0.18 \pm 0.06$	[2]	$0.40 \pm 0.01$	[2]
$q = M_2/M_{\text{BH}}$	$0.079 \pm 0.007$	[3]	$0.024 \pm 0.009$	[2]	$0.06 \pm 0.004$	[4]
$a$ ( $R_{\odot}$ )	$5.49 \pm 0.32$	[1]	$2.54 \pm 0.06$	[2]	$3.79 \pm 0.04$	[2,5]
$R_2$ ( $R_{\odot}$ )	$1.06 \pm 0.07$	[1]	$0.34 \pm 0.05$	[2]	$0.67 \pm 0.02$	[2,5]
$P_{\text{orb}}$ (day)	0.432605(1)	[6]	0.16993404(5)	[2]	0.32301415(7)	[2]
$\dot{P}_{\text{orb}}$ ( $\text{ms yr}^{-1}$ )	$-20.7 \pm 12.7$	[6]	$-1.90 \pm 0.57$	[2]	$-0.60 \pm 0.08$	[2]
$T_{\text{eff}}$ (K)	$4400 \pm 100$	[3]	$4700 \pm 100$	[8]	$4900 \pm 100$	[7]
	4065-5214	[9]	3405-4640	[9]	3800-4910	[9]

<sup>a</sup> Meanings of the parameters:  $M_{\text{BH}}$  - the BH mass,  $M_2$  - the donor mass,  $q$  - the mass ratio,  $a$  - the semi-major axis of the orbit,  $R_2$  - donor's radius,  $P_{\text{orb}}$  - the orbital period,  $\dot{P}_{\text{orb}}$  - the changing rate of the orbital period,  $T_{\text{eff}}$  - the effective temperature of the donor.

<sup>b</sup> References: [1] Wu et al. (2016); [2] González Hernández et al. (2014); [3] Wu et al. (2015); [4] Neilsen, Steeghs & Vrtilik (2008); [5] González Hernández et al. (2011); [6] González Hernández et al. (2017); [7] González Hernández et al. (2004); [8] González Hernández et al. (2006); [9] Fragos & McClintock (2015)

**Table 2.** Selected initial parameters for the BHLMBs

Parameter	Nova Muscae 1991	XTE J1118+480	A0620-00
$M_2$ ( $M_{\odot}$ )	1	1.0	1
$M_{\text{BH}}$ ( $M_{\odot}$ )	11	6.6	6
$P_{\text{orb}}$ (day)	1.5	1.65	1.72

**Table 3.** Input parameters ( $\alpha$ ,  $r_0$ ,  $t_{\text{vis},0}$ ,  $M_{\text{CB},0}$ )

	A0620-00	XTE J1118+480	Nova Muscae 1991
upper row	(0.1, $10a$ , 1 yr, $4 \times 10^{24}$ g)	(0.1, $10a$ , 1 yr, $4 \times 10^{24}$ g)	(0.1, $10a$ , 1 yr, $4 \times 10^{25}$ g)
middle row	(0.01, $10a$ , 10 yr, $4 \times 10^{25}$ g)	(0.01, $10a$ , 10 yr, $4 \times 10^{25}$ g)	(0.01, $10a$ , 10 yr, $4 \times 10^{26}$ g)
lower row	(0.1, $100a$ , 30 yr, $12.8 \times 10^{24}$ g)	(0.1, $100a$ , 30 yr, $12.8 \times 10^{24}$ g)	(0.1, $100a$ , 30 yr, $12.8 \times 10^{25}$ g)

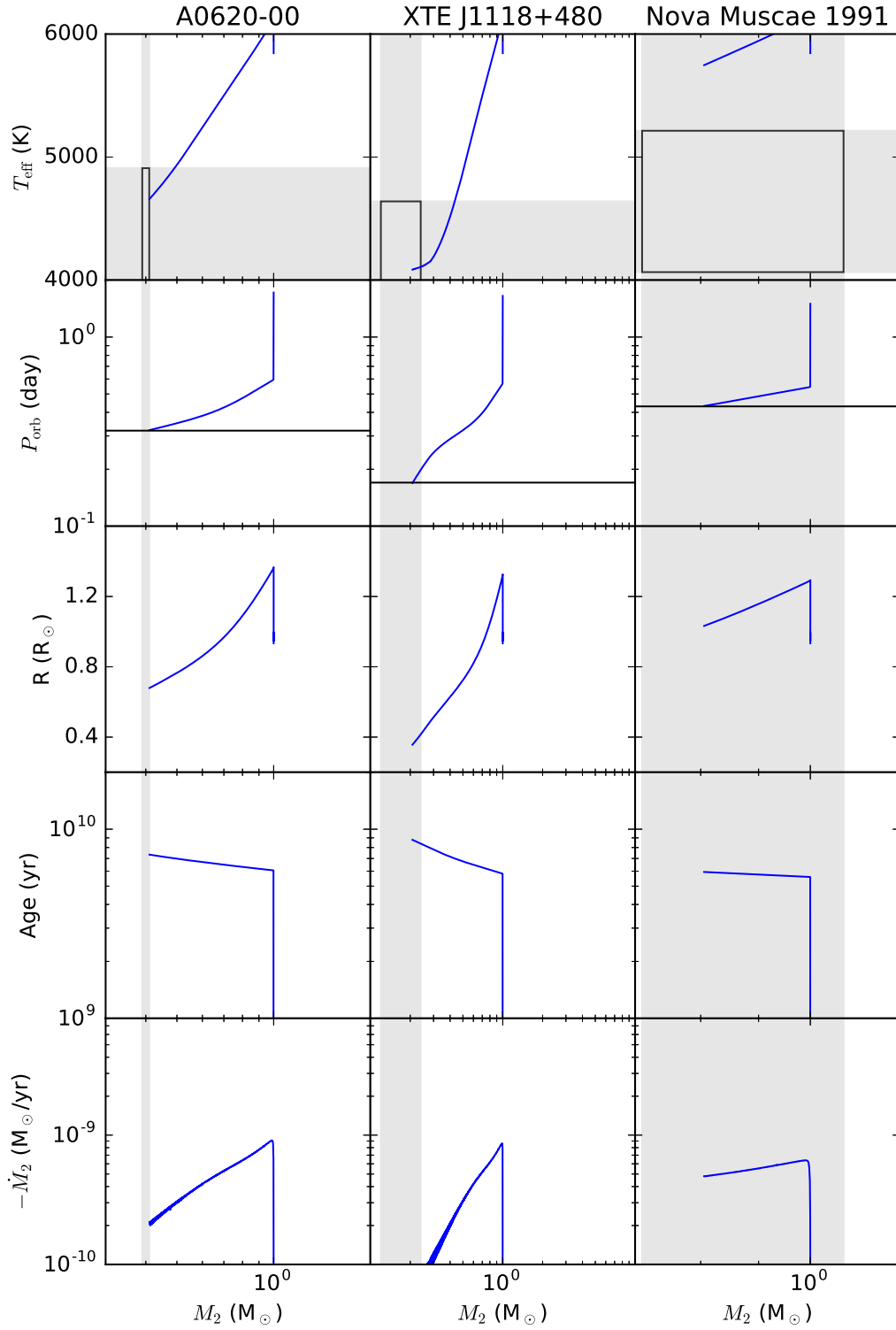


**Figure 1.** The pre-CB disk evolution for the three BHLMBXBs. The blue solid lines represent the evolutionary tracks, and the shaded areas represent the observational constraints.

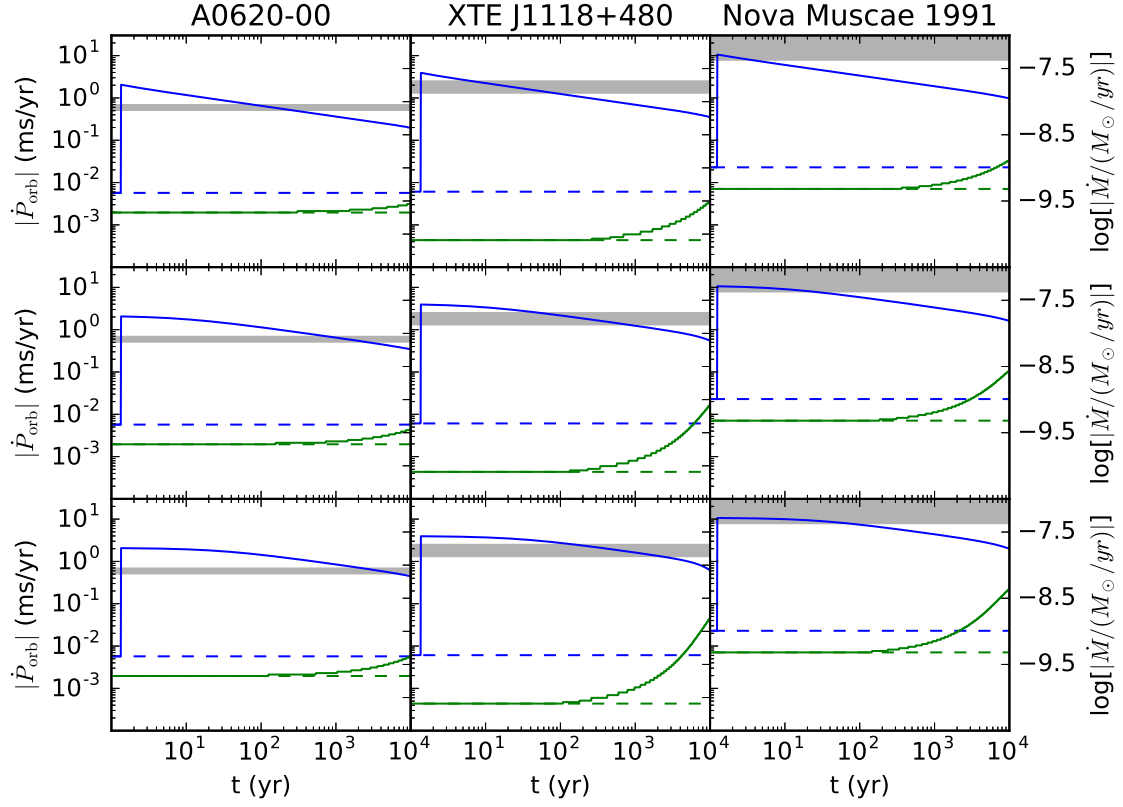


**Figure 2.** The evolution for the three BHLMXBs with a CB disk fed by single outburst with  $n = 1/4$ . The input parameters ( $\alpha$ ,  $r_0$ ,  $t_{\text{vis},0}$ ,  $M_{\text{CB},0}$ ) are listed in Table 3. The blue and green solid lines represent the evolution of  $|\dot{P}_{\text{orb}}|$  and  $|\dot{M}_2|$ , respectively. The dashed lines show the evolution in the absence of the CB disk for comparison. The shaded areas represent the observed range of  $|\dot{P}_{\text{orb}}|$ .

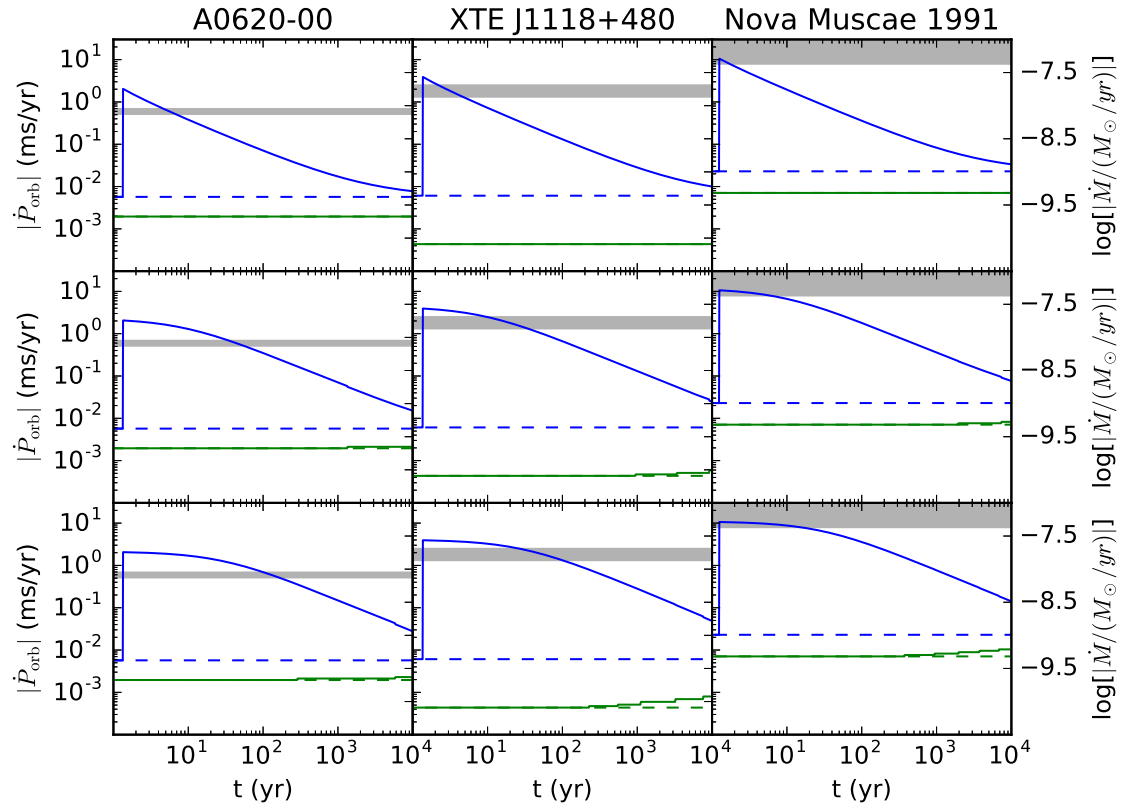


**Figure 3.** Same as Fig. 2 but for  $n = 3/4$ .

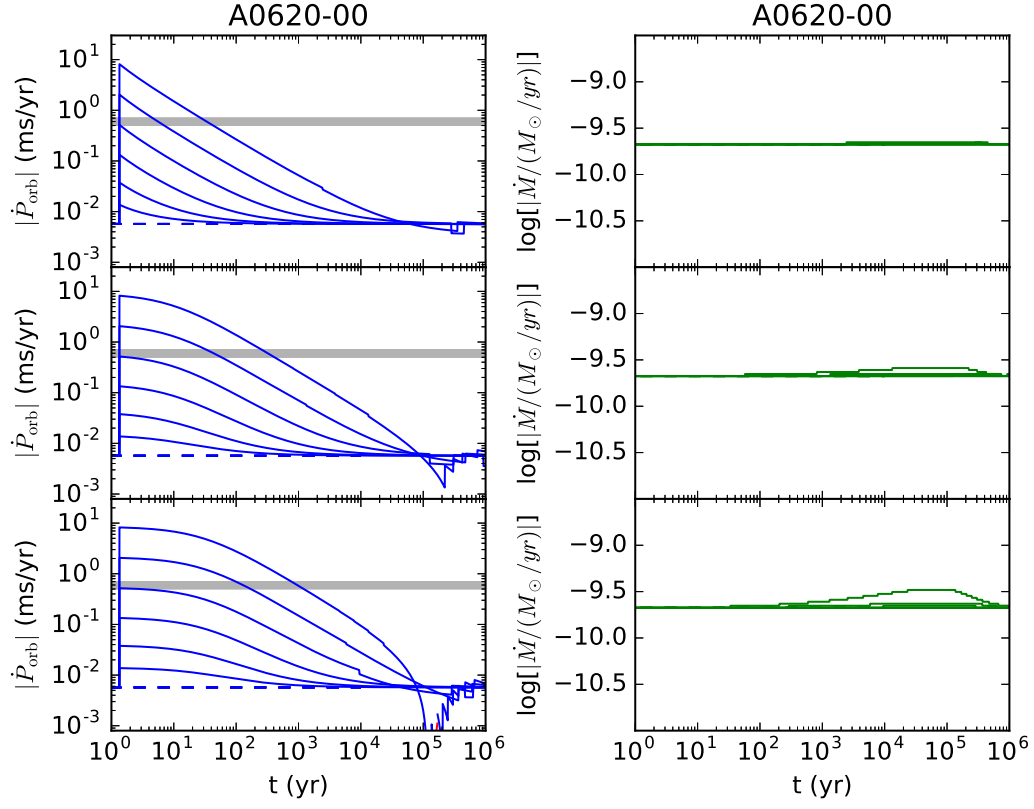


**Figure 4.** The evolution with a CB disk for A0620-00. In each panel the solid curves from top to bottom are obtained with  $\zeta = (4, 1, 4^{-1}, 4^{-2}, 4^{-3}, 4^{-4})$ , respectively. Other symbols have the same meanings as in Fig. 2.

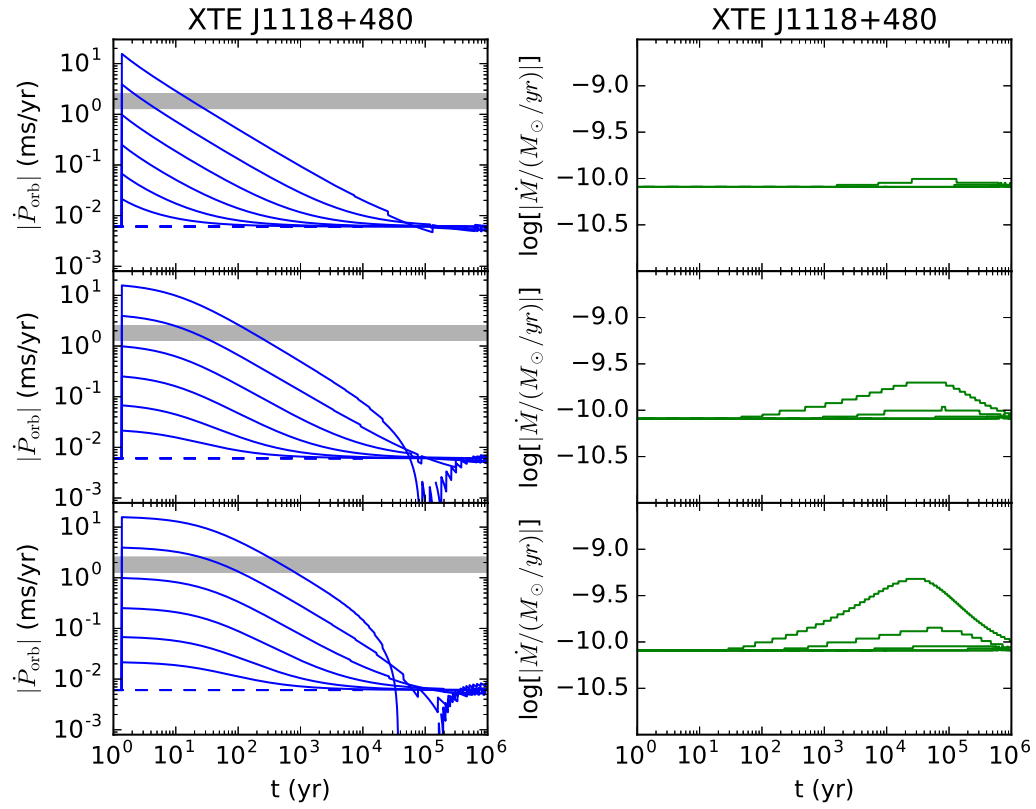


**Figure 5.** Same as Fig. 4 but for XTE J1118+480.

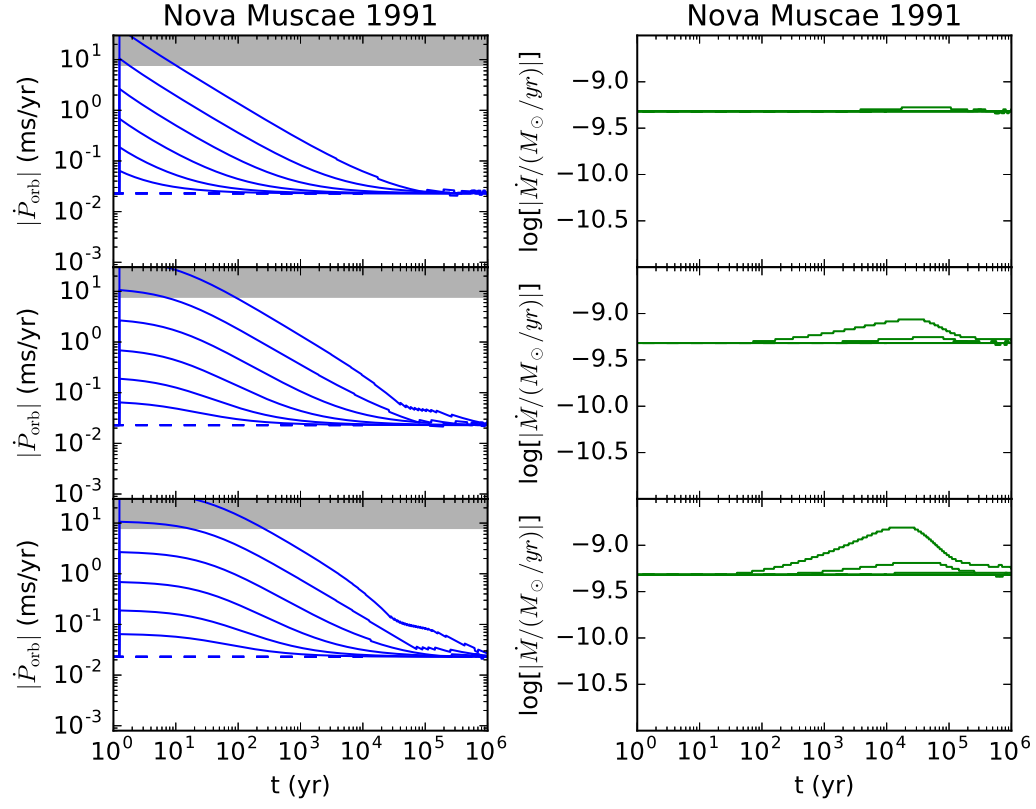


**Figure 6.** Same as Fig. 4 but for Nova Muscae 1991.

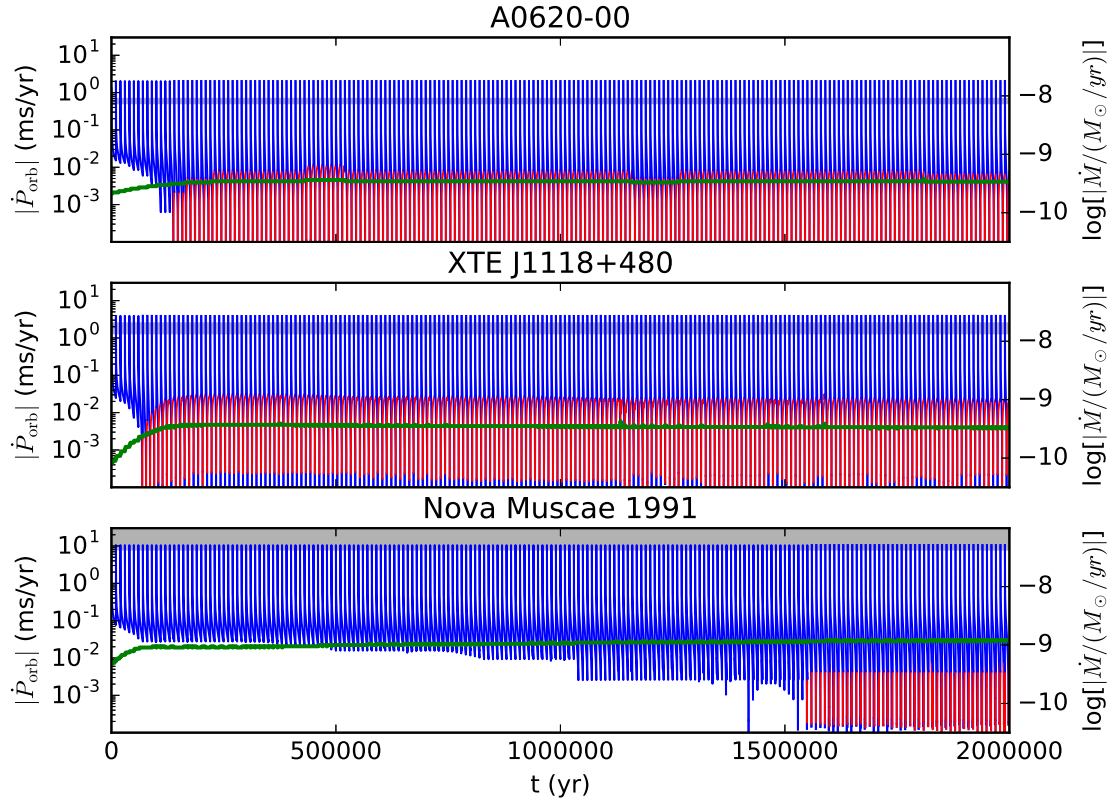


**Figure 7.** The evolution with a CB disk fed by repeating outbursts. Other symbols have the same meanings as in Fig. 2.

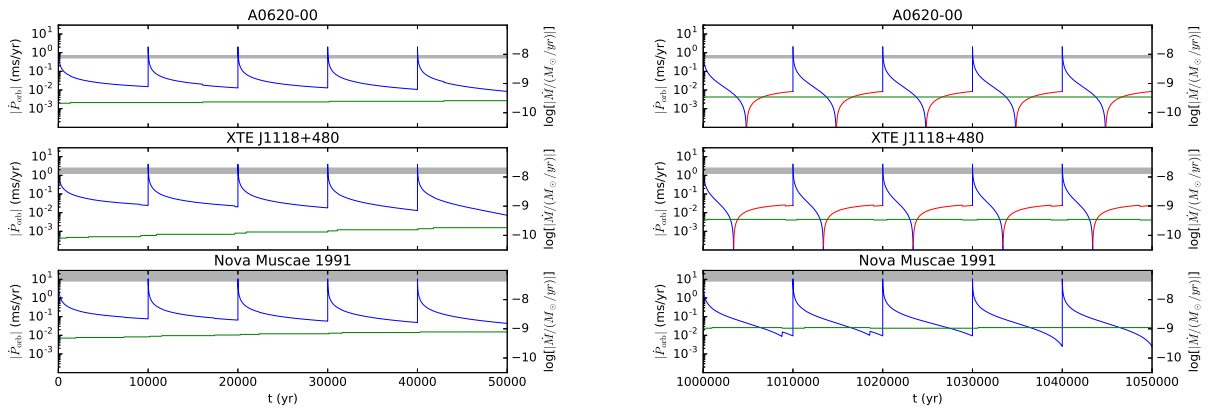


**Figure 8.** Zoom in of Fig. 7 during the time 0 - 50000 yr (left) and  $10^6$  yr -  $(10^6 + 50000)$  yr (right).

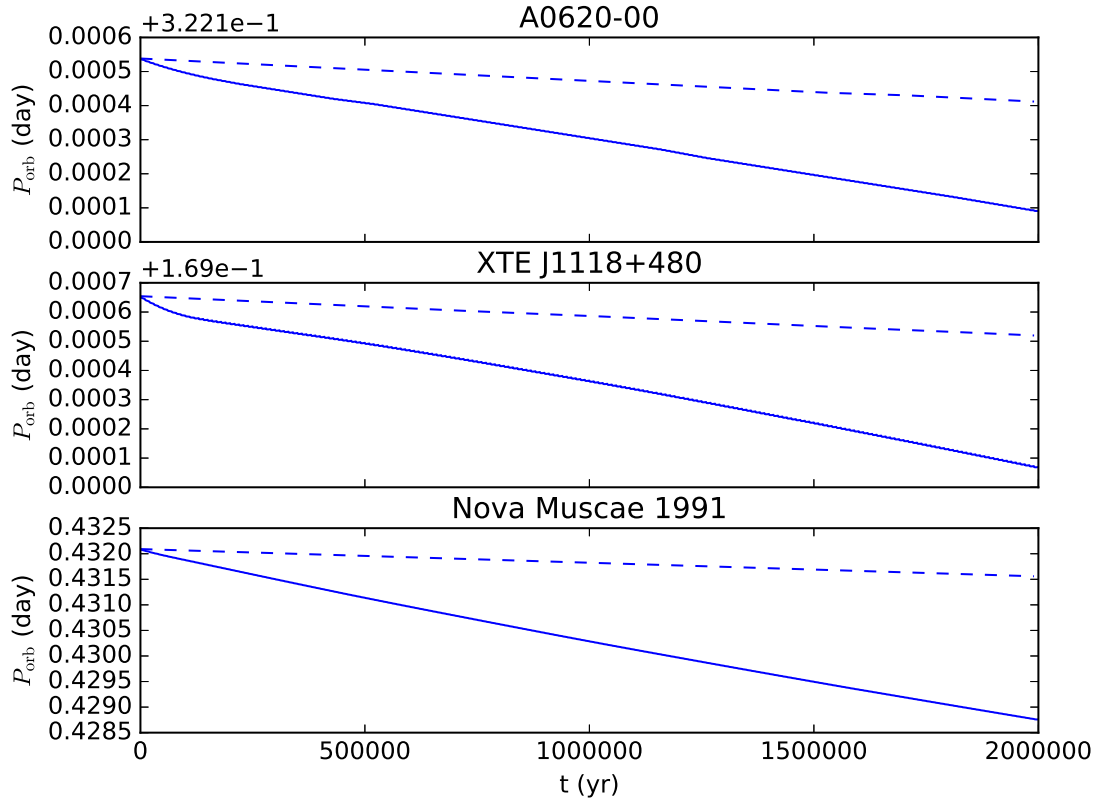


**Figure 9.** Comparison of the long-term orbital evolution with and without a CB disk, depicted with the solid and dashed lines, respectively.